

Tracing Presolar Grain Populations Through Matrix Alteration Histories. N. D. Nevill¹⁻³, A. N. Nguyen², E. G. Alevy⁴, K. A. McCain⁵, T. M. Erickson⁵ and L. P. Keller². ¹Lunar and Planetary Institute, Universities Space Research Association, 3600 Bay Area Blvd., Houston, Texas, 77058 USA, ²Astromaterials Research and Exploration Science, NASA Johnson Space Center, 2101 NASA Parkway, Mail Code XI3, Houston, TX 77058, USA, ³Space Science and Technology Centre, School of Earth and Planetary Sciences, Curtin University, Australia, ⁴Department of Geology, Colby, USA College, ⁵Jacobs JETSII contract, NASA Johnson Space Center.

Introduction: Primitive meteorites preserve remnants of evolved stars as presolar grains, from asymptotic and red giant branch stars, novae and supernovae. These grains retain records of the formation mechanisms of the stellar environment from which they condensed, as well as physical and chemical processes in the interstellar medium (ISM), solar nebula and the parent bodies in which they are found. Consequently, their study can refine our understanding of the solar system and external stellar and planetary systems [1]. However, presolar grains and their records can be altered, re-equilibrated with the surrounding matrix, and eventually lost through aqueous and thermal processing on the meteorite parent body [2].

NanoSIMS is the most rapid and effective method for *in situ* identification of presolar grains via their highly anomalous isotopic ratios [1]. Previous studies have measured variations in presolar grain populations between different matrix regions within the same meteorite thin section. However, most of these studies do not identify if there are any ties between these variations in presolar grain populations and the chemical and mineralogical differences in measured matrix regions [1]. Therefore, the goal of this study is to determine if there is measurable variations in the degree of alteration of different matrix regions within the same thin section, and if mineralogical and chemical changes in matrix regions can be used as indicators for presolar grain preservation.

Such a correlation could improve the efficiency of presolar grain identification during searches across large surface areas. To do this, we carried out coordinated scanning electron microscope (SEM) and NanoSIMS analyses, using a new SEM method which measures the ppm concentration of 100 nm to 5 μm sized Mg-, S-, Al-, C- and Ca-rich matrix grains.

Approach and Methods: We studied polished thin sections of DOM 08006 (CO3), ALH 77307 (CO), EET 83226 (C2-Ung) and MIL 090019 (CO3) for their bulk matrix compositions and presolar grain populations at the Astromaterials Research and Exploration Science (ARES), Johnson Space Centre (JSC), NASA.

Secondary electron, backscattered electron, , and energy dispersive spectroscopy (EDS) chemical images were collected using a JEOL 7900F scanning electron microscope (SEM) equipped with an Oxford Instruments Ultim Max SDD X-ray detector. Context

maps were collected at 15 kV for initial thin section characterisation and selection of target matrix regions. The latter were chosen based on their (1) area, (2) distance from each other within the thin section, (3) proximity to the outer edge ($\geq 100 \mu\text{m}$ away) and (4) the number of fragmented inclusions distributed amongst selected matrix regions. All SEM data were processed using Oxford Instruments AZtec software.

EDS analyses of targeted matrix regions were conducted with operating conditions of 15kV accelerating voltage, 4 nA current, and a working distance of 9.0 mm. The higher beam current reduced the spot size to enable measurements of major element abundances of matrix grains down to $\sim 100 \text{ nm}$, and longer dwell times improved the accuracy of the measurements. This method enabled us to determine the average surface area of Mg-, S-, Al-, C- and Ca-rich phases within each measured matrix region and calculate their overall concentration in ppm. The concentrations of these elements are affected by thermal and aqueous alteration on the parent body [3-5].

The average surface area of Mg-, S-, Al- and Ca-rich phases in each matrix region was calculated using ImageJ software. All noise and large inclusions ($\geq 20 \mu\text{m}$) were removed from the image before calculating the abundances of Mg-, S-, Al- and Ca-rich mineral phases in ppm. The concentration of Fe-rich phases was not calculated as they were ubiquitous within each matrix region, and Mg is considered a more effective measure of changes in alteration [5].

Isotopic O and C imaging was conducted using the Cameca NanoSIMS 50L at NASA JSC. Ion images of $^{12}\text{C}^-$, $^{13}\text{C}^-$, $^{16}\text{O}^-$, $^{17}\text{O}^-$, $^{18}\text{O}^-$, $^{28}\text{Si}^-$, and $^{40}\text{Ca}^{16}\text{O}^-$ were obtained with $\sim 100 \text{ nm}$ spatial resolution by rastering a focused 0.8 pA Cs^+ primary ion beam over $20 \mu\text{m} \times 20 \mu\text{m}$ regions for over three hours. Prior to analysis, each acquisition region was pre-sputtered with a 200 pA Cs^+ primary ion beam to remove the conductive Pt coat and implant Cs. San Carlos olivine and USGS graphite were used as isotopic standards for O and C analyses respectively.

Results: A total of 39 matrix regions were mapped using SEM-EDX across the four thin sections. The average matrix grain sizes were 100 to 500 nm. Of the regions analyzed by SEM, three were measured using NanoSIMS for presolar grain populations in MIL 090019, with areas of $11,625 \mu\text{m}^2$, $15,820 \mu\text{m}^2$, and

8,130 μm^2 [6]. Two regions each were mapped by NanoSIMS in DOM 08006 and EET 83226, with total areas of 8,352 μm^2 (DOM Region 1), 6,505 μm^2 (DOM Region 2), 2,665 μm^2 (EET Region 1) and 8,817 μm^2 (EET Region 2). Five regions with areas 1,915 μm^2 , 6,334 μm^2 , 7,957 μm^2 , 2,219 μm^2 and 1,901 μm^2 were mapped in ALH 77307.

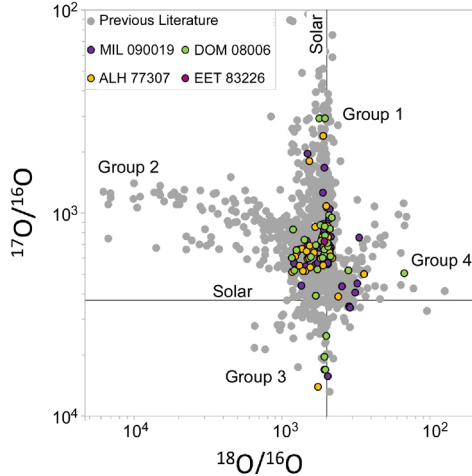


Figure 1. Oxygen isotopic compositions of O-rich presolar grains in MIL 090019 [6], ALH 77307, DOM 08006 and EET 83226 Vs. presolar oxides and silicates from [7].

Presolar grains were identified in all matrix regions, with 61 O-rich grains in MIL 090019 [6], 32 O-rich grains in DOM 08006, 1 O-rich grain in EET 83226 and 36 O-rich grains in ALH 77307 (Figure 1). The lower abundance of presolar silicates identified in EET 83226 was attributed to the higher abundance of bulk carbonaceous material in this meteorite. EET 83226 is classified as C2-ung with affinities to CO meteorites and a carbon content similar to CM meteorites [8].

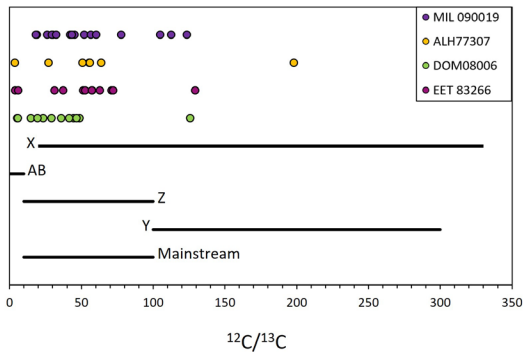


Figure 2. Carbon isotopic compositions of C-rich presolar grains in MIL 090019 [6], ALH 77307, DOM 08006 and EET 83226 Vs. presolar SiC types [1]. Presolar graphites have similar compositional ranges to SiC.

A total of 16 C-Rich presolar grains were identified in MIL 090019 [6], 12 in DOM 08006, 12 in EET 83266

and 7 in ALH 77307. These grains were primarily SiC. Their isotopic compositions are shown in Figure 2.

Discussion: Measurable variations in matrix composition were found when analysing ppm concentrations of Mg-, S-, Al- and Ca-rich phases between matrix regions. Al showed the least variation amongst different regions while Mg, Ca and S varied significantly. Figure 3 illustrates the relationship between the mineralogical and geochemical variations and presolar grain populations within 3 different matrix regions in MIL 090019. Higher concentrations of C-rich presolar grains are associated with higher concentrations of S. In contrast Al appears to decrease in concentration with larger C-rich presolar populations. A similar relationship is seen between Ca, Mg and O-rich presolar grain populations with Mg concentrations increasing with increasing O-rich presolar grain populations and Ca decreasing. While not depicted, higher bulk carbonaceous content was associated with a decrease in presolar O-rich phases. The Ca-rich phases and its distribution throughout the matrix indicate aqueous fluids were most prominent within regions with the lowest presolar grain populations, as supported by the reduction of Mg-rich phases. Results indicate measurable variations are present amongst different matrix regions and can be used as indicators for presolar grain populations.

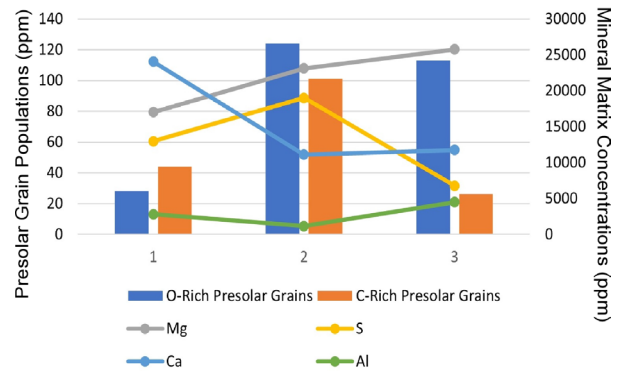


Figure 3. O- and C-rich presolar grain abundances (ppm) plotted against the abundance of Mg-, S-, Al- and Ca-rich phases within each matrix region (ppm) for ALH 77307 and MIL 090019.

References: [1] Zinner E. (2014) in *Meteorites and cosmochemical processes*, 1, (eds. A. Davis) 181–213. [2] Trigo-Rodriguez, J. M., and Blum, J. (2008) *PASA* 26(3), 289-296. [4] Floss C. and Stadermann F. (2009) *Geochim. Cosmochim. Acta.*, 2415-2440. [5] Brearley A. J. (2006) *Meteorites and the early solar system II*, 587-624. [6] Seifert L. B. et al. (2023) *Met. Planet. Sci.*, 58(3), 360-382. [7] Nguyen A. N. et al. (2021) *LPSC 52*, #2709. [8] Hynes K.M. and Gyngard F. (2009) *LPSC XL*, Abstract #1198.